Published in final edited form as:
J Phys Chem B. 2011 February 24; 115(7): 1608–1615. doi:10.1021/jp109764f.

Optically Transparent Recombinant Silk-Elastinlike Protein Polymer Films

Weibing Teng[†], **Yiding Huang**[†], **Joseph Cappello**[‡], and **Xiaoyi Wu**[*,†,§]

[†] Department of Aerospace and Mechanical Engineering, University of Arizona, Tucson, Arizona 85721, United States

[‡] Protein Polymer Technologies, Inc., San Diego, California 92121, United States

[§] Biomedical Engineering Program & Bio5 Institute, University of Arizona, Tucson, Arizona 85721, United States

Abstract

Recombinant protein polymers, evaluated extensively as biomaterials for applications in drug delivery and tissue engineering, are rarely reported as being optically transparent. Here we report the notable optical transparency of films composed of a genetically engineered silk-elastinlike protein polymer SELP-47K. SELP-47K films of 100 μm in thickness display a transmittance of 93% in the wavelength range of 350–800 nm. While covalent cross-linking of SELP-47K via glutaraldehyde decreases its transmittance to 77% at the wavelength of 800 nm, noncovalent cross-linking using methanol slightly increases it to 95%. Non- and covalent cross-linking of SELP-47K films also influences their secondary structures and water contents. Cell viability and proliferation analyses further reveal the excellent cytocompatibility of both non- and covalently cross-linked SELP-47K films. The combination of high optical transparency and cytocompatibility of SELP-47K films, together with their previously reported outstanding mechanical properties, suggests that this protein polymer may be useful in unique, new biomedical applications.

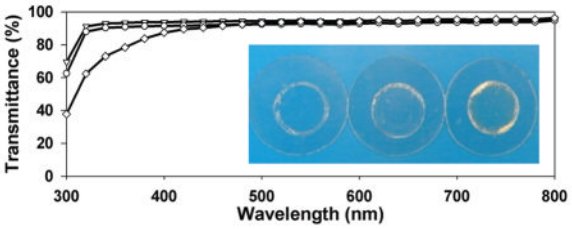

INTRODUCTION

Genetic engineering of recombinant proteins provides material scientists with high levels of control over material structure, property, and function.[1] Many polypeptide sequences, which are derived from natural proteins such as silk[2] and elastin,[3] have been used as motifs for the biosynthesis of recombinant protein polymers. The resulting protein polymers often inherit some structure and property characteristics from their parent proteins. For instance, elastinlike proteins display the elasticity characteristics of native elastin,[4–6] and silklike

[*]Corresponding Author: Tel.: 1-00-520-626-5854. Fax: 1-00-520-621-8191. xwu@email.arizona.edu.

Supporting Information. Images of water droplets on nontreated SELP-47K films; soluble fractions of SELP-47K protein films; transmittance of nontreated and MeOH-GTA-treated films of different thicknesses. This material is available free of charge via the Internet at http://pubs.acs.org.

proteins form β-sheet crystals that are responsible for the high tensile strength and fracture toughness of native silks.[7,8] Moreover, multiblocked protein copolymers in which individual blocks may possess distinct mechanical, chemical, or biological properties have been bio-synthesized.[9–11] As an example, silk-elastin like protein (SELP) polymers consisting of silklike and elastinlike polypeptide sequences have been produced[11] and fabricated into various structures, such as microdiameter fibers and nanofibrous scaffolds, displaying unique mechanical properties that combine high deformability, tensile strength, and resilience.[12–14] The potential of protein polymers for applications in drug delivery[15–17] and tissue engineering[2,3] is being extensively investigated. However, optical transparency of materials composed of recombinant protein polymers has rarely been reported.

Optically transparent polymers have many important applications. For instance, poly(hydroxyethyl methacrylate) is the primary polymer used in the fabrication of contact lenses. Additionally, poly(dimethylsiloxane) (PDMS) has been widely used for fabricating microfluidic devices, due to its optical transparency, mechanical robustness, and ease of processing.[18,19] PDMS[20] and silicone rubber[21,22] have also been used as cell culture substrates; their optical transparency permits real-time observations and analyses of the cellular and subcellular processes, such as the assembly and disassembly of focal adhesions. However, for these applications because they are biologically inert, PDMS and silicone rubber substrates need to be coated with extracellular matrix (ECM) proteins in order to promote cell attachment. In contrast, recombinant protein polymers often display enhanced biocompatibility, promoting cell-material interactions. Moreover, specific functional groups, such as the RGD and CS5 cell binding domains of fibronectin, can be readily incorporated into SELP[23] and elastinlike protein polymers.[24] However, recombinant protein polymers remain largely unknown for their optical transparency. Interestingly, silk fibroin proteins from silkworms were recently processed into transparent thin films, although silk fiber is not transparent.[25]

We hypothesize that materials composed of silklike proteins and block protein polymers containing silklike sequences may be rendered optically transparent by controlling or limiting the size and the chemical nature of their interchain cross-links. In this work, the optical properties of an SELP-47K protein polymer with a monomer structure of $(S)_4(E)_4(EK)(E)_3$, in which S is the silklike sequence GAGAGS (one-letter amino acid abbreviation), E is the elastinlike sequence GVGVP, and EK is the pentapeptide sequence GVGKP, were examined. It is noteworthy that the silklike sequence GAGAGS in SELP-47K is the canonical sequence found in silkworm silk fibroin. The silklike sequence is capable of crystallizing to provide the SELP-47K structures non-covalent cross-linking and mechanical strength. Although the spontaneous crystallization of the silklike sequences in aqueous solution is relatively slow,[26] it can be greatly accelerated by methanol or other nonsolvents.[12,13] An alternative stabilization strategy of SELP-47K is covalent cross-linking. The lysine residues present in SELP-47K permit chemical cross-linking of the elastinlike blocks using glutaraldehyde.[12–14] Effects of the covalent and noncovalent cross-linking on the light transmittance of SELP-47K films were examined. In addition, the cytocompatibility of SELP-47K films was analyzed.

MATERIALS AND METHODS

Sample Preparation

Frozen SELP-47K (884 amino acid chain length; MW69 814) aqueous solution at a concentration of 13 w/w% was generously provided by Protein Polymer Technologies, Inc. (San Diego, CA). The complete amino acid sequence of SELP-47K was previously reported,[11] while its purity and molecular weight were examined by MALDI-TOF and SDS-PAGE in our recent study.[12] The SELP-47K solution was lyophilized and redissolved in deionized

(DI) water at a concentration of 200 mg/mL at room temperature. The protein solution was mixed thoroughly by vortex, and air bubbles were removed by centrifugation prior to use.

Optical Characterization

SELP-47K films of 20 to 100 μm in thickness were prepared by casting the protein solution on coverslips. The solvent was evaporated at room temperature under ambient conditions. Film thickness was controlled by the amount of protein solution used in the sample preparation and measured by a Dektak 150 Surface Profiler (Veeco). Some cast films were treated with 99.9% methanol (MeOH) (Fisher Scientific) for 24 h prior to air-drying, and denoted as MeOH-treated films. Following an established protocol,[12,27] some MeOH-treated films were cross-linked using 1% (w/v) glutaraldehyde (GTA) (Mallinckrodt Baker) solutions for 24 h, and denoted as MeOH-GTA-treated films. The MeOH-GTA-treated films were extensively rinsed using DI water and air-dried under ambient conditions. Following a protocol detailed elasewhere,[28,29] three types of SELP-47K films, including non-, MeOH-, and MeOH-GTA-treated samples, were optically analyzed. Briefly, a dry or hydrated sample was taped to a sample holder with the sample facing the incident beam, and transmittance was measured using a Cary 5000 UV/vis-NIR spectrometer (Varian). The transmittance of glass coverslips without any film sample was also measured. A method was established to subtract the minimal effect of the coverslip from the transmittance measurement of SELP-47K films. Hydrated samples were prepared by wetting thin films in DI water, equilibrating overnight, and blotting away any excess water.

SELP-47K thin films (5-μm thick) were also cast on SiO_2 wafer under ambient conditions. Following the same MeOH and GTA treatments, the refractive index (RI) of non-, MeOH-, and MeOH-GTA-treated films was determined using a Metricon prism coupler (Metricon) at wavelength 532, 632.8, and 1554 nm, respectively.[30] SELP-47K films on SiO_2 wafers were brought into contact against the base of the prism to ensure the coupling between the sample and prism surfaces. The measurements were performed on three to five replicates of each type of SELP-47K film.

Water Contact Angles

To evaluate the hydrophilicity of SELP-47K films, contact angles of non-, MeOH-, and MeOH-GTA-treated samples cast on SiO_2 wafer were detected employing drops of DI water (5 μL) using Easy Drop DSA20B (Kruss),[31] and determined by analyzing the optical images of droplets using the sessile drop fitting algorithm.32 Measurements were performed on five to seven replicates of each type of SELP-47K film.

Surface Roughness

Because surface roughness greatly affects contact angle measurements,[33] atomic force microscopy (AFM) was performed on non-, MeOH-, and MeOH-GTA-treated samples cast on SiO_2 wafer to determine their surface roughness. The AFM images were acquired in triplicate under the tapping mode using a MultiMode AFM (Digital Instruments) equipped with an NSC-15 tapping mode cantilever (Figure 1). The associated AFM software NanoScope was used to calculate the mean surface roughness of each type of film (Table 1). The surface roughness of the SiO_2 wafer is around 0.115 nm.[34]

Secondary Structural Analysis

The SELP-47K aqueous solution was poured into polypropylene casting molds and the solvent evaporated at room temperature under ambient conditions. The resulting films were peeled off the mold surface, obtaining free-standing films for further MeOH and GTA treatments. Three types of SELP-47K films, including non-, MeOH-, and MeOH-GTA-

treated films, were analyzed using Raman and Fourier transform infrared (FTIR) spectroscopy. Briefly, a Magna-IR 560 Nicolet spectrometer (Madison, WI) equipped with a CsI beam splitter, DTGS-detector, and OMNIC software was used to record IR spectra. Dry air free of CO_2 was used to continuously purge the spectrometer to eliminate CO_2 and H_2O absorbance. For each sample, 400 scans were collected over the spectral range of 4000–650 cm^{-1} at a resolution of 4 cm^{-1}. Likewise, Raman spectra of SELP-47K films were recorded on a Thermo Nicolet Almega micro Raman system (Thermo Scientific). A solid-state laser with the wavelength of 532 nm was used as the excitation source. Due to the strong fluorescent effects that have been reported in GTA-fixed tissues and cells,[35] the Raman spectrum of MeOH-GTA-treated films was not obtainable.

FTIR spectra of SELP-47K films in the spectral range of 1720–1580 cm^{-1} were smoothed with a 9-point smooth Savitzky-Golay function on GRAMS 8.0 and fitted with Gaussian band profiles. A baseline subtraction was also performed on GRAMS 8.0, and all of the FTIR spectra were normalized by the areas of the amide I bands. Following a procedure established by Taddei and Monti,[36] the secondary-derivative and self-deconvolution methods were used to identify individual characteristic bands of the broadened amide I bands. All three types of films displayed the same individual characteristic bands. Areas under individual bands normalized by the total area of the amide I band represent the percentage contents of secondary structures of SELP-47K films. Specifically, the band at 1616 cm^{-1} was assigned to aggregated strands, while bands at 1624, 1635, 1675, and 1695 cm^{-1} were assigned to β-sheet and sheet like structure.[36] Bands at 1662 and 1684 cm^{-1} were assigned to β-turns. Bands at 1646 and 1653 cm^{-1} were assigned to irregular structures, including random coils and extended chains.

Equilibrium Swelling

The swelling behavior of free-standing MeOH- and MeOH-GTA-treated SELP-47K films was evaluated in DI water containing 0.2 mg/mL NaN_3 to prevent biological contamination. The DI water was changed several times over a time period of 72 h, ensuring the removal of the dissolved protein polymer. After gently removing excess water, the weight of swollen films (W_s) was measured every 24 h until samples reached equilibrium (<1% change in weight in 24 h). Dry films were obtained by placing swollen films in a vacuum oven at 60 °C. After being equilibrated to room temperature in a desiccator, dry films were weighted and placed back in the oven. The weight of dry films (W_d) was measured every 24 h until the difference between two consecutive measurements was less than 1%. Each measurement was performed in triplicate. The equilibrium swelling ratio (q) and water content (H) of the SELP-47K films were determined using the following formulas:[37–39]

$$q = W_s / W_d \tag{1}$$

$$H = (1 - W_d / W_s) \times 100\% \tag{2}$$

Mechanical Analysis

Free-standing MeOH- and MeOH-GTA-treated SELP-47K films were cut into rectangular samples with dimensions of 15 × 2 mm for mechanical analyses. The gauge length was 6.0 mm. Samples were hydrated in 1 × phosphate buffered saline (PBS) containing 0.2 mg/mL NaN_3 at 37 °C. The hydrated film thickness, typically 0.2 mm, was measured by optical microscopy.[14] Mechanical characterization of SELP-47K samples was performed using a Perkin-Elmer diamond DMA, and samples were immersed in a jacketed beaker filled with 1

× PBS at 37 °C. Both MeOH- and MeOH-GTA-treated films were evaluated by uniaxial tensile stress–strain analysis. Five replicate samples of each type of film were monotonically extended to failure so the deformability and ultimate tensile strength were obtained. Displacement was applied at a fixed rate of 0.25 mm/min. The Young's modulus of a sample was determined as the slope of the stress–strain curve in the first 40% deformation region.

Cell Viability

Both MeOH- and MeOH-GTA-treated SELP-47K films along with coverslips were sterilized by immersion in 70% ethanol overnight. Following a protocol detailed elsewhere,[14] 230 μL of NIH/3T3 fibroblast suspension in DMEM containing 10% FBS at a cell density of 300 cells/μL was added onto each film, and incubated in an incubator at 37 °C with 5% CO_2 until cells reached 100% confluence. Fresh media were exchanged each 3 days. On day 5, the viability of cells grown on the MeOH- and MeOH-GTA-treated films was examined using a LIVE/DEAD Viability/Cytotoxicity Kit (Invitrogen).

Cell Proliferation

The proliferation of cells cultured on the MeOH- and MeOH-GTA-treated SELP-47K films with coverslips was analyzed by the MTS assay (Promega) on days 1, 3, 5, and 7. The initial cell seeding density was 10 000 cells/cm^2. Live cells react with a tetrazolium salt in the MTS reagent, producing a soluble formazan dye, which has an absorbance at a wavelength of 490 nm. Within the linear region of the absorbance curve, the number of cells is proportional to the absorbance intensity, measured using a Nanodrop UV–vis spectrophotometer (Thermo Scientifc). After each SELP-47K film with cells was retrieved, it was placed into 200 μL of medium containing 40 μL of MTS reagent, and incubated for 2 h prior to measurement of the absorbance intensity at 490 nm. As a control, cells were also cultured in a tissue culture polystyrene (TCPS) well without SELP-47K film.

Statistical Analysis

Cell viability and proliferation were analyzed in at least triplicate, and measurements were expressed as mean ± standard deviation (SD). Student's *t* test (SigmaPlot) was employed to assess statistical significance of the results. Differences were considered statistically significant at $p < 0.05$.

RESULTS AND DISCUSSION

UV–vis spectroscopy reveals that SELP-47K thin films (30 μm thickness) are optically transparent to visible light but opaque to ultraviolet (UV) light (Figure 2 and Figure S2 of the Supporting Information). Transmittances of non- and MeOH-treated films decrease slightly from 95% at 800 nm to 92% and 90% at 350 nm, respectively. Transmittances of MeOH-GTA-treated films decrease from 96% at 800 nm to 91% at 450 nm, and then to 75% at 350 nm. Considering variation in sample thickness and experimental error, all three types of SELP-47K thin films display comparable transparency at wavelengths of 800–450 nm. The low optical transparency of SELP-47K films at wavelengths below 350 nm is likely due to strong UV absorption by the SELP-47K polypeptide. Indeed, UV absorption at 280 nm is routinely used to quantify protein concentration. GTA cross-linking intensifies the UV absorption of SELP-47K films. GTA is known to react with and modify the amines of collagen and other proteins, leading to UV absorption at 300 and 325 nm.[40,41] This likely explains the lower transparency of MeOH-GTA-treated films in the near-UV region, as compared to that of non- and MeOH-treated films.

The influence of film thickness on the optical transparency of non- and covalent cross-linking SELP-47K films was assessed using thicker samples (average thickness of 92 μm; Figure 3). Nontreated films displayed transmittances of 90% at 800 nm, 88% at 450 nm, and 85% at 350 nm. At the same wavelengths, MeOH-treated films possessed transmittances of 93%, 90%, and 88%, while MeOH-GTA-treated films showed transmittances of 77%, 66%, and 37%, respectively. Again, in these thicker films, noncovalent cross-linking via methanol does not compromise the optical transparency of SELP-47K films. In contrast, considerable reduction (i.e., about 20%) in the transmittance of MeOH-treated SELP-47K films is induced by covalent cross-linking using GTA. Moreover, MeOH-GTA-treated films appear to be slightly yellowish (Figure 2, insert).

The physical properties of hydrated recombinant protein polymers are more relevant than dry ones to many biomedical applications. Interestingly, hydration slightly improves the optical transparency of all three types of SELP-47K films to visible light, resulting in a 2–6% increase in their transmittance (Figure 3). Hydrated non- and MeOH-treated films display nearly identical transmittances at all wavelengths from 800 to 300 nm. Although the underlying mechanism still remains poorly understood, hydration was reported to greatly enhance the optical transparency of upper cortices of *L. pulmonaria*.42 In contrast, the anticancer drug Tamoxifen, which induced dehydration in the lens of the eye, impaired lens clarity.[43] We speculate that hydration changes the interfacial properties of protein microstructures including our SELP-47K films, thereby attenuating light scattering and reflection. In our previous study, scanning electron microscopy (SEM) revealed the microfibrillar structures of SELP-47K films, which were formed by protein globules of micrometer sizes.[12] According to the hierarchical self-assembly model proposed by Jin and Kaplan for silk,44 those micrometer protein globules may be formed by micelles of 100–200 nm in size. The micro/nanofibrils and microgobules undoubtedly create numerous microinterfaces within SELP-47K films. Light deflection and scattering at these interfaces may account for the slight reduction of optical transparency of SELP-47K films. This is analogous to reduction in the optical transparency of glass by internal cracks. However, hydration changes the microinterfaces of SELP-47K films from air/protein into water/protein, probably leading to reduction in light deflection/scattering and improvement in film transparency.

The equilibrium swelling ratio and the extent of hydration of MeOH- and MeOH-GTA-treated SELP-47K films were analyzed in DI water (Table 2). When fully hydrated, a MeOH-treated film absorbed approximately 100% of its weight in water, while a MeOH-GTA-treated film absorbed water up to 62% of its weight. As a result, hydrated MeOH- and MeOH-GTA-treated films contained 51% (w/w) and 38% (w/w) water, respectively. It is worth noting that hydration only marginally increased the dimensions of SELP-47K films, e.g., less than 5% in length and width. Likely, most of the absorbed water filled the existing micro and nanopores of the dry SELP-47K films. The swelling ratios of SELP-47K films are much lower than SELP-47K hydrogels (e.g., 8 to 9).[36] The major difference between SELP-47K films and hydrogels resides in the fabrication process and their resulting microstructures. When casting films, the complete evaporation of solvent (e.g., DI water) enhances the interactions between the polymer chains, leading to the formation of intra- and inter-molecular hydrogen bonds and the irreversible crystallization of the silklike blocks that greatly stabilize the films. This speculation is supported by little, if any, removal of the soluble fractions of both MeOH- and MeOH-GTA-treated films (Figure S3 of the Supporting Information). In contrast, the solvent retained when SELP-47K hydrogels are cured results in less crystallization of the silklike blocks. This would explain the significant differences between the swelling ratios of SELP-47K films and hydrogels.

Nontreated SELP-47K films are not mechanically stable after hydration in DI water.[12] Indeed, droplets placed on the nontreated films for contact angle measurement were quickly absorbed by the film surface (Figure S1 of the Supporting Information). As a result, the contact angles of nontreated films was initially 36.2 ± 4.4°, but quickly reduced to 11.9 ± 2.2° when the droplets stabilized on the sample surface after about 1 min. In contrast, MeOH- and MeOH-GTA-treated films were stable in water. Their contact angles were 67.8 ± 2.2° and 64.1 ± 3.7°, respectively, which are similar to those of contact lens materials such as Asmoficon (71.2 ± 1.5°), Balafison (71.5 ± 1.1°), and Enfilcon (68.3 ± 1.5°).[45]

Mechanical properties of MeOH- and MeOH-GTA-treated SELP-47K films were examined using uniaxial tensile stress–strain analysis. Fully hydrated MeOH-treated films possessed an ultimate tensile strength of 2.5 ± 0.4 MPa and a strain at failure of 190 ± 60% (Figure 4). MeOH-GTA-treated films displayed enhanced mechanical properties, including ultimate tensile strength (5.4 ± 1.1 MPa) and strain to failure (245 ± 58%). Young's modulus of MeOH- and MeOH-GTA-treated films, estimated in the first 40% strain, were 1.57 ± 0.3 and 3.17 ± 0.23 MPa, respectively. Together with the equilibrium swelling data, glutaraldehyde cross-linking not only reduces the water content of MeOH-treated films, but also improves their mechanical properties.

The optical transparency of SELP-47K films displayed weak thickness dependence. When the film thickness increased from 18 to 97 μm, a moderate reduction of 3% in transmittance was observed in hydrated MeOH-treated films (Figure 5). Increasing the thickness of nontreated films resulted in a similar reduction in transmittance (Figure S4 of the Supporting Information). MeOH-GTA-treated films showed a stronger dependence of optical transparency on thickness. When their thicknesses increased from 16 to 92 μm, a 17% loss of optical transparency was observed (Figure S5 of the Supporting Information). This is consistent with the fact that GTA cross-linking induced more absorbance of SELP-47K films at all wavelengths. The thickness-dependent transmittance (T) of SELP-47K films can be described by Beer's law, $T = 10^{-\alpha l}$, where α is the attenuation coefficient and l is the film thickness. Linear regression was used to obtain the attenuation coefficients of hydrated SELP-47K films (Table 3). Non- and MeOH-treated films displayed comparable attenuation coefficients at 450 and 350 nm. The attenuation coefficient of MeOH-GTA-treated films was much higher than that of non- and MeOH-treated films at the same wavelengths, suggesting a more pronounced reduction in transparency when their thickness increased.

Listed in Table 4 are the refractive indices (RI) of non-, MeOH-, and MeOH-GTA-treated films measured at 532, 632.8, and 1552 nm, respectively. The RI of SELP-47K films were similar to those of PMMA (1.490 ± 0.001),46 Etafilcon A (1.412 ± 0.0017),47 and Lotrafilcon B (1.424 ± 0.0003),47 which were measured at 589 nm.

The influence of cross-linking on the secondary structures of SELP-47K films was analyzed using Raman and FTIR spectroscopy. Silk-based materials often exist in two distinct crystalline forms: silk I and silk II. Silk I comprises less-ordered conformations such as β-turns.[48,49] In contrast, silk II largely consists of well-defined antiparallel β-sheets. In a Raman spectrum, a silk II structure displays marker bands at 1230 cm^{-1} (amide III), 1085 cm^{-1} (CC skeletal stretching and $C(CH_3)_2$ rocking), 971 cm^{-1} (CH_3 rocking), and 878 cm^{-1} (CC and CN stretching). [50,51] Likewise, Raman marker bands for a silk I structure include 1248, 1102, 954, and 856 cm^{-1}. A Raman analysis of nontreated SELP-47K films revealed Raman marker bands of a silk I structure (Figure 6). After MeOH treatment, SELP-47K films displayed Raman marker bands for silk II. In particular, the amide III shifted from 1248 to 1230 cm^{-1}, and the CC skeletal stretching shifted from 1102 to 1085 cm^{-1}, suggesting that methanol treatment induced a conversion from silk I to silk II. The silk I to II conversion resulted in the formation of more packed, insoluble antiparallel β-sheets. As a

result, the mechanical properties of SELP-47K films were significantly improved.[12] Our current work shows the MeOH-treatment induced conformational conversion slightly improves the excellent optical transparency of SELP-47K films (Figure 3). Nevertheless, the existence of weak Raman marker bands for silk I in MeOH-treated films, including shoulders at 1248 and 1102 cm^{-1} and weak bands at 954 and 856 cm^{-1} (Figure 6), indicates an incomplete conversion from silk I to silk II.

In contrast to the unambiguous detection of the silk II conversion by Raman spectroscopy, FTIR analysis of SELP-47K films was less distinctive. The amide I band of nontreated films appeared at 1630 cm^{-1}, typical of antiparallel β-sheets (Figure 7A). Still, the breadth of the amide I band indicated the coexistence of other conformations. The amide I band of methanol-treated films at 1617 cm^{-1} suggested the formation of aggregated stands, likely a consequence of strong intermolecular hydrogen bonding.[52] Infrared bands characteristic of silk I at 1410 cm^{-1} ($C_\alpha H_2$ stretching36) and 1330 cm^{-1} (CH_3 symmetric stretching36) were displayed by nontreated films and disappeared or were weakened after methanol treatment (Figure 7B). In contrast, the band intensity at 1070 cm^{-1}, typical of silk II, increased after methanol treatment (Figure 7C). Because GTA likely reacts with only one lysine of every 64 amino acid residues of the SELP-47K monomer, the FTIR spectral changes in the amide I and III regions after GTA cross-linking should appear to be very subtle, if not negligible (Figure 7A,B). Spectral changes were more pronounced in the regions of the CC skeletal stretching vibrations (Figure 7C). In particular, bands of ordered helix at 928 and 912 cm^{-1} nearly disappeared, indicating that GTA cross-linking disrupted ordered helical conformations of SELP-47K films. Additionally, a band at 1070 cm^{-1} attributable to the CC skeletal stretching of silk II intensified after methanol treatment, but weakened after GTA cross-linking.

Quantitative structural information on SELP-47K films was derived by curve fitting of the FTIR amide I bands with Gaussian band profiles (Figure 7A, Table 5). Although Taddei and Monti did not differentiate aggregated strands from β-sheets for silk fibroin,[36] our recent mechanical analysis of SELP-47K films suggests that it is useful to distinguish the two conformations. [12] Specifically, nontreated films did not display significant mechanical strength and were unstable when hydrated in water, while MeOH-treated films possessed excellent mechanical strength and retained material integrity in water. Indeed, methanol treatment increased the content of aggregated strands from 22% to 38%, at the expense of β-sheets and unordered structures. Aggregated β-strands, which are more extensively hydrogen-bonded, but are not necessarily more ordered than antiparallel β-sheets, likely provide more robust physical cross-links and thus higher tensile strength to SELP-47K films. A moderate disruption of the β-sheet and sheet like structure was also observed in MeOH-treated films upon glutaraldehyde cross-linking, resulting in slight gains in aggregated β-strands, β-turns, and unordered structures after glutaraldehyde cross-linking. This was consistent with the qualitative analysis of the weak FTIR spectra ascribed to the CC skeletal stretching, which suggested a slight increase in silk I at the expense of silk II.

An ideal biomaterial should be biocompatible with cell attachment, proliferation, and other cellular functions. In this work, the NIH/3T3 fibroblasts were used as amodel system to evaluate the in vitro cytocompatibility of SELP-47K films. Cell viability was assessed using the LIVE/DEAD assay. After staining, live cells produce an intense green fluorescence while dead cells emit a bright red fluorescence. The cell viability assay revealed that the cells seeded and grown on both types of SELP-47K films for 5 days were substantially viable (Figure 8A,B). Cell viability was quantified by counting the number of live cells versus the total cells in ten digital fluorescence images of stained cells on each type of film. The percent viabilities of 3T3 fibroblasts on MeOH- and MeOH-GTA treated films were 97.2 ± 2.0% and 99.6 ± 0.5%, respectively.

To evaluate the ability of SELP-47K films to support cell proliferation, NIH/3T3 fibroblasts were seeded at the same density on MeOH- and MeOH-GTA-treated films and in TCPS wells as a control. Their proliferation profiles were assessed using the MTS assay. During a period of 7 days, fibroblasts cultured on SELP-47K films continuously grew in number (Figure 9). Both scaffolds demonstrated cell proliferation comparable to the culture control on TCPS. Together with the viability assays, the proliferation study shows that SELP-47K films display excellent cytocompatibility.

CONCLUSIONS

The genetically engineered silk-elastinlike protein polymer SELP-47K in the form of thin films displays excellent transmittance in the wavelength range of 350–800 nm. While GTA cross-linking of the films results in a moderate reduction in transmittance, noncovalent cross-linking via MeOH treatment retains the high optical transparency of SELP-47K films to visible light. When fully hydrated, an MeOH-treated film of 97-μm thickness possesses a transmittance of 96%. This verifies that recombinant protein polymers containing the silklike sequence can be formed in thin films with good optical transparency. Raman and FTIR spectroscopic analysis further reveals the conformational conversion of SELP-47K films from Silk I to II structures and the formation of aggregated β-strands upon methanol treatment. Robust physical cross-links formed by the aggregated β-strands likely provide MeOH-treated films with the previously reported mechanical properties that are comparable to those of native soft tissues, in contrast to the lack of mechanical strength of nontreated films. Last, the LIVE/DEAD and cell proliferation assays demonstrate the high in vitro cytocompatibility of SELP-47K films. We plan to study the applications of SELP-47K films in opthalmic applications such as contact lenses, synthetic corneas, intraocular lenses, and opthalmic drug delivery matrixes and as cell culture substrates in the study of cellular and subcellular activities.

Supplementary Material

Refer to Web version on PubMed Central for supplementary material.

Acknowledgments

This research was supported by NIBIB (R21EB009160) and NSF (CMMI0856215).

References

1. van Hest JCM, Tirrell DA. Chem Commun 2001:1897.
2. Altman GH, Diaz F, Jakuba C, Calabro T, Horan RL, Chen JS, Lu H, Richmond J, Kaplan DL. Biomaterials 2003;24:401. [PubMed: 12423595]
3. Welsh ER, Tirrell DA. Biomacromolecules 2000;1:23. [PubMed: 11709838]
4. Meyer DE, Chilkoti A. Nat Biotechnol 1999;17:1112. [PubMed: 10545920]
5. Wright ER, Conticello VP. Adv Drug Delivery Rev 2002;54:1057.
6. Lee TAT, Cooper A, Apkarian RP, Conticello VP. Adv Mater 2000;12:1105.
7. Szela S, Avtges P, Valluzzi R, Winkler S, Wilson D, Kirschner D, Kaplan DL. Biomacromolecules 2000;1:534. [PubMed: 11710178]
8. Winkler S, Wilson D, Kaplan DL. Biochemistry 2000;39:12739. [PubMed: 11027155]
9. Petka WA, Harden JL, McGrath KP, Wirtz D, Tirrell DA. Science 1998;281:389. [PubMed: 9665877]
10. Wu XY, Sallach R, Haller CA, Caves JA, Nagapudi K, Conticello VP, Levenston ME, Chaikof EL. Biomacromolecules 2005;6:3037. [PubMed: 16283724]

11. Cappello J, Crissman JW, Crissman M, Ferrari FA, Textor G, Wallis O, Whitledge JR, Zhou X, Burman D, Aukerman L, Stedronsky ER. J Controlled Release 1998;53:105.
12. Teng WB, Cappello J, Wu XY. Biomacromolecules 2009;10:3028. [PubMed: 19788307]
13. Qiu WG, Teng WB, Cappello J, Wu XY. Biomacromolecules 2009;10:602. [PubMed: 19186950]
14. Qiu WG, Huang YD, Teng WB, Cohn CM, Cappello J, Wu XY. Biomacromolecules 2010;11:3219. [PubMed: 21058633]
15. Meyer DE, Shin BC, Kong GA, Dewhirst MW, Chilkoti A. J Controlled Release 2001;74:213.
16. Haider M, Megeed Z, Ghandehari H. J Controlled Release 2004;95:1.
17. Pardridge WM. Bioconjugate Chem 2008;19:1327.
18. Duffy DC, McDonald JC, Schueller OJA, Whitesides GM. Anal Chem 1998;70:4974.
19. McDonald, JcC; Whitesides, GM. Acc Chem Res 2002;35:491. [PubMed: 12118988]
20. Balaban NQ, Schwarz US, Riveline D, Goichberg P, Tzur G, Sabanay I, Mahalu D, Safran S, Bershadsky A, Addadi L, Geiger B. Nat Cell Biol 2001;3:466. [PubMed: 11331874]
21. Harris AK, Wild P, Stopak D. Science 1980;208:177. [PubMed: 6987736]
22. Lee J, Leonard M, Oliver T, Ishihara A, Jacobson K. J Cell Biol 1994;127:1957. [PubMed: 7806573]
23. Anderson JP, Cappello J, Martin DC. Biopolymers 1994;34:1049. [PubMed: 8075387]
24. Heilshorn SC, DiZio KA, Welsh ER, Tirrell DA. Biomaterials 2003;24:4245. [PubMed: 12853256]
25. Lawrence BD, Marchant JK, Pindrus MA, Omenetto FG, Kaplan DL. Biomaterials 2009;30:1299. [PubMed: 19059642]
26. Hwang W, Kim BH, Dandu R, Cappello J, Ghandehari H, Seog J. Langmuir 2009;25:12682. [PubMed: 19803470]
27. Bigi A, Cojazzi G, Panzavolta S, Rubini K, Roveri N. Biomaterials 2001;22:763. [PubMed: 11246944]
28. Drummy LF, Koerner H, Phillips DM, McAuliffe JC, Kumar M, Farmer BL, Vaia RA, Naik RR. Mater Sci Eng, C 2009;29:1266.
29. Kharlampieva E, Kozlovskaya V, Gunawidjaja R, Shevchenko VV, Vaia R, Naik RR, Kaplan DL, Tsukruk VV. Adv Funct Mater 2010;20:840.
30. Hattori T, Shibata T, Onodera S, Kaino T. J Appl Phys 2000;87:3240.
31. Lorentz H, Rogers R, Jones L. Optom Vis Sci 2007;84:946. [PubMed: 18049360]
32. Amirfazli A, Graham-Eagle J, Pennell S, Neumann AW. Colloids Surf, A 2000;161:63.
33. Tamai Y, Aratani K. J Phys Chem 1972;76:3267.
34. Teichert C, Mackay JF, Savage DE, Lagally MG, Brohl M, Wagner P. Appl Phys Lett 1995;66:2346.
35. Collins JS, Goldsmith TH. J Histochem Cytochem 1981;29:411. [PubMed: 6787116]
36. Taddei P, Monti P. Biopolymers 2005;78:249. [PubMed: 15800959]
37. Dinerman AA, Cappello J, Ghandehari H, Hoag SW. Biomaterials 2002;23:4203. [PubMed: 12194523]
38. Lee J, Macosko CW, Urry DW. Macromolecules 2001;34:4114.
39. Domb A, Davidson GWR, Sanders LM. J Controlled Release 1990;14:133.
40. Cheung DT, Nimni ME. Connective Tissue Res 1982;10:187.
41. Cheung DT, Nimni ME. Connective Tissue Res 1982;10:201.
42. Gauslaa Y, Solhaug KA. Oecologia 2001;126:462.
43. Zhang JJ, Jacob TJC, Valverde MA, Hardy SP, Mintenig GM, Sepulveda FV, Gill DR, Hyde SC, Trezise AEO, Higgins CF. J Clin Invest 1994;94:1690. [PubMed: 7929848]
44. Jin HJ, Kaplan DL. Nature 2003;424:1057. [PubMed: 12944968]
45. Read ML, Morgan PB, Maldonado-Codina C. J Biomed Mater Res, Part B 2009;91B:662.
46. Tranoudis I, Efron N. Contact Lens Ant Eye 1998;21:15.
47. Varikooty J, Keir N, Woods CA, Fonn D. Eye Contact Lens 2010;36:2. [PubMed: 20009942]
48. Asakura T, Ashida J, Yamane T, Kameda T, Nakazawa Y, Ohgo K, Komatsu K. J Mol Biol 2001;306:291. [PubMed: 11237601]

49. Asakura T, Yao JM, Yamane T, Umemura K, Ultrich AS. J Am Chem Soc 2002;124:8794. [PubMed: 12137522]
50. Monti P, Taddei P, Freddi G, Asakura T, Tsukada M. J Raman Spectrosc 2001;32:103.
51. Zheng SD, Li GX, Yao WH, Yu TY. Appl Spectrosc 1989;43:1269.
52. Jackson M, Mantsch HH. Crit Rev Biochem Mol Biol 1995;30:95. [PubMed: 7656562]

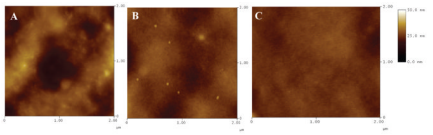

Figure 1.
AFM images of non-(A), MeOH-(B), and MeOH-GTA-treated SELP-47K films (C).

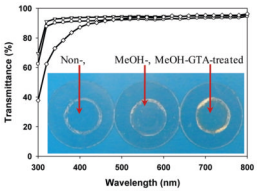

Figure 2.
Transmittance of non-(▽), MeOH-(○), and MeOH-GTA-treated (◇) SELP-47K dry films of 30 μm thickness. Measurements were done in triplicate. Insert: photo images of SELP-47K films cast on coverslips.

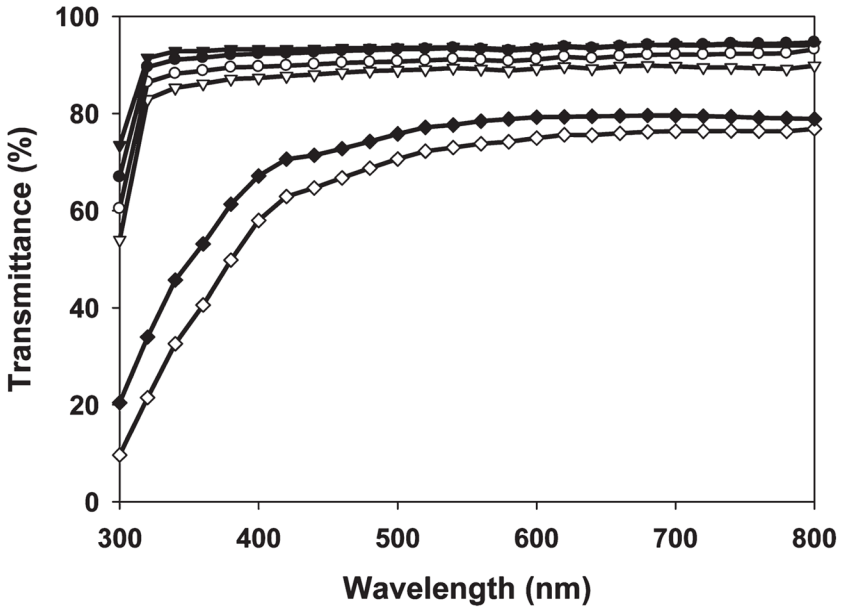

Figure 3.

Hydration effects on the optical transparency of non-(▽ ▼), MeOH-(○●), and MeOH-GTA-treated (◇◆) SELP-47K films of 92 μm thickness (dry film thickness). Measurements were done in triplicate. Dry samples (▽ ○ ◇); hydrated samples (▼ ● ◆).

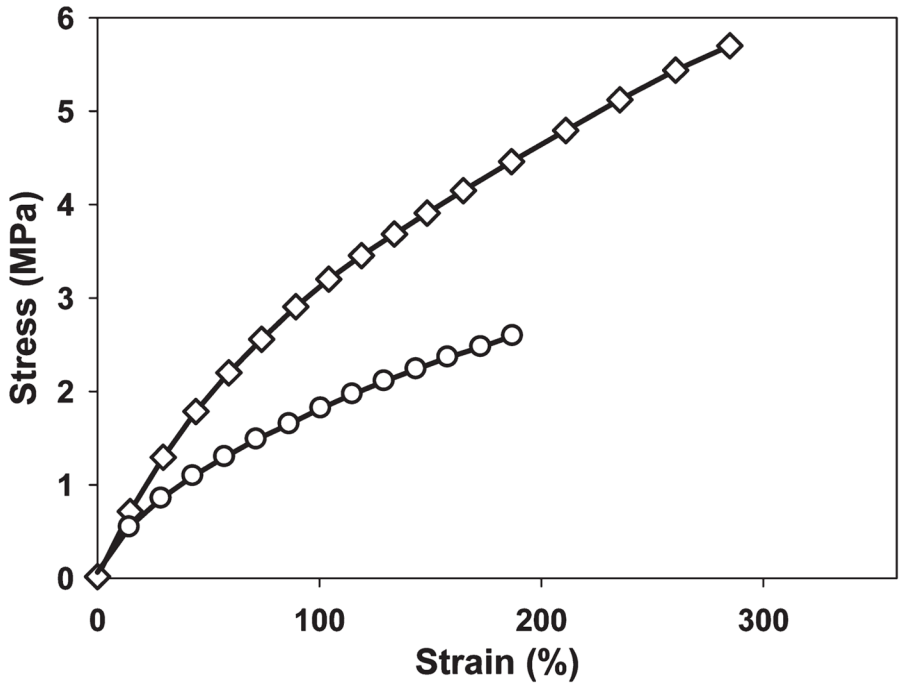

Figure 4.
Representative uniaxial stress–strain analysis of fully hydrated MeOH-(○), and MeOH-GTA-treated (◇) SELP-47K films. Measurements were done on five replicate film samples of each type.

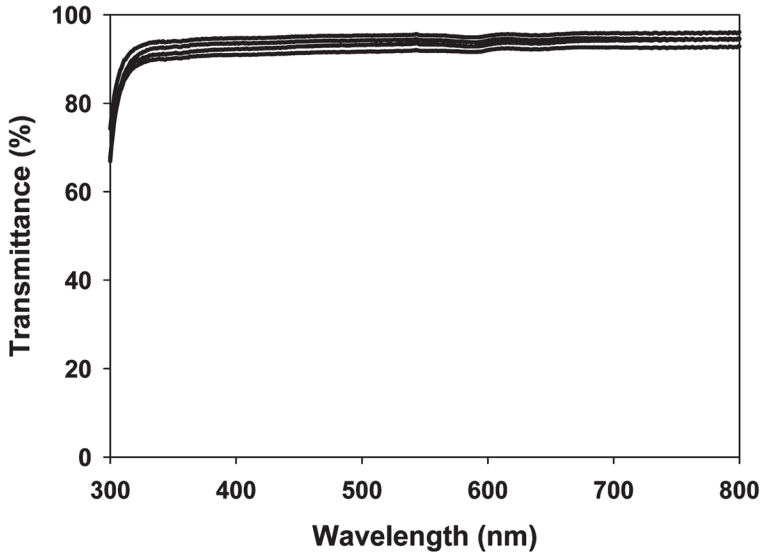

Figure 5.
Transmittance of hydrated MeOH-treated SELP-47K films of various thicknesses, 18, 30, 56, and 97 μm (from top to bottom). Data represent measurements of 3 samples per film.

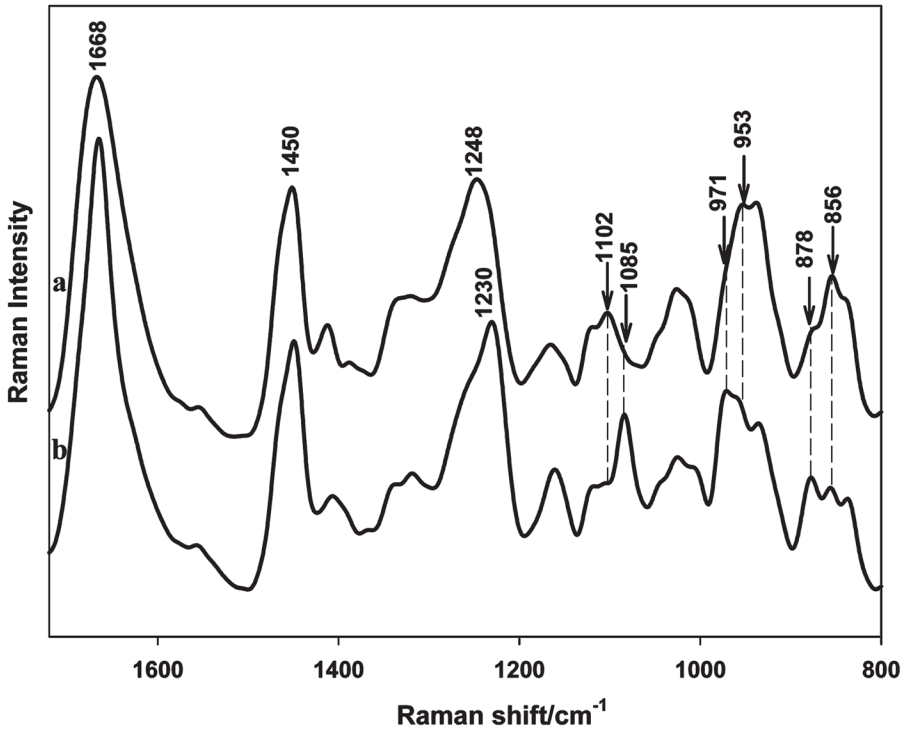

Figure 6.
Raman spectra of non-(a) and MeOH-treated (b) SELP-47K films in the spectral range of 1720–800 cm^{-1}.

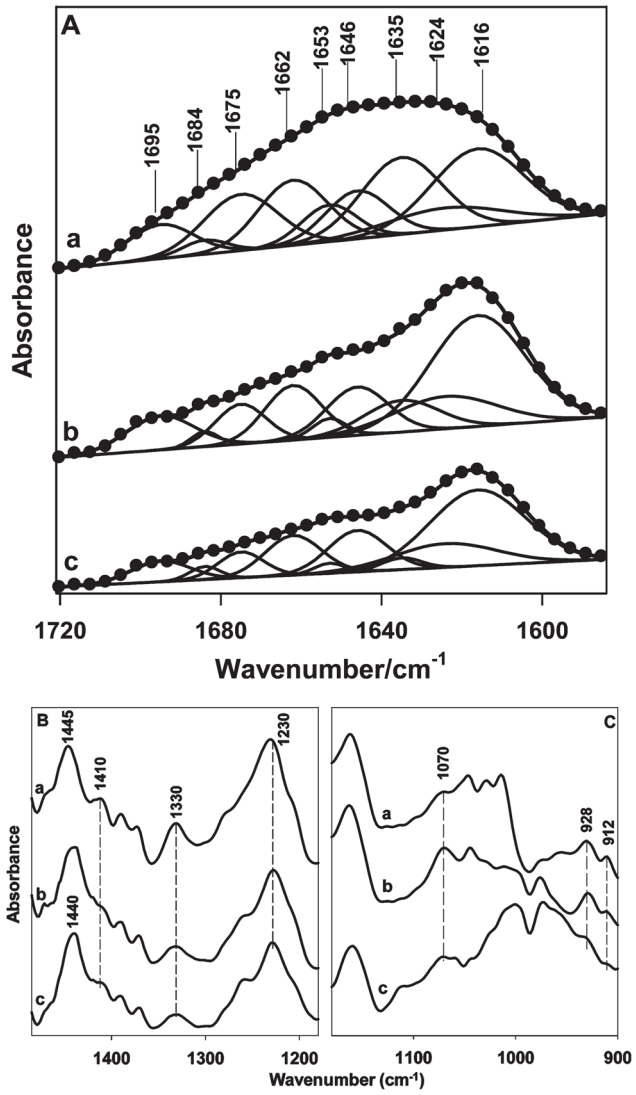

Figure 7.

(A) FTIR amide I spectra were fitted with Gaussian band profiles; (B) and (C) FTIR spectra in the spectral range of 1490–900 cm^{-1}: non-(a), MeOH-(b), and MeOH-GTA-treated (c) SELP-47K films. The spectra were intensified by about 10-fold in (C).

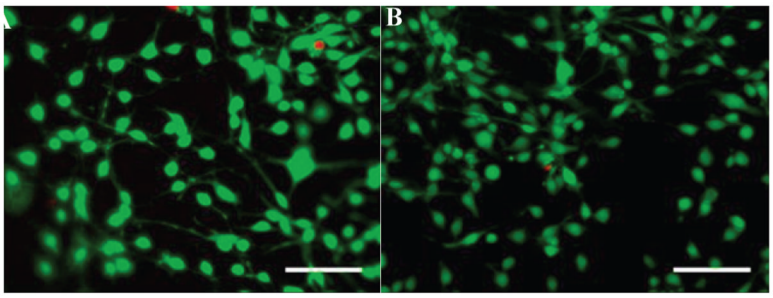

Figure 8.
Fluorescent staining for cell viability of NIH/3T3 fibroblasts grown on MeOH-(A) and MeOH-GTA-treated (B) SELP-47K films on day 5. Living cells are in green and dead cells are in red. Scale bars: 100 μm.

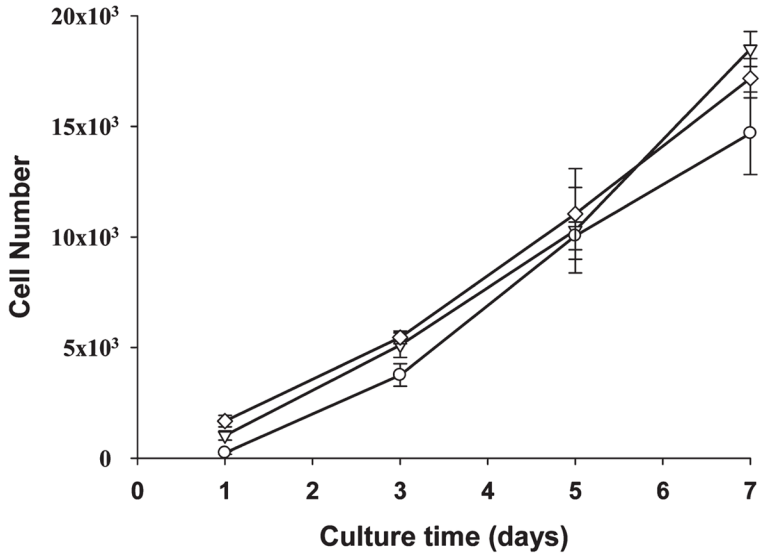

Figure 9.

Proliferation profiles of 3T3 fibroblasts grown on TCPS wells (▽, as control), MeOH-treated (○) and GTA-cross-linked (◇) SELP-47K films up to 7 days. Data and error bars represent measurements conducted on triplicate culture wells.

Table 1

Mean Surface Roughness Values of Non-, MeOH-, and MeOH-GTA-Treated Films

	nontreated	MeOH-treated	MeOH-GTA-treated
mean surface roughness (nm)	1.485 ± 0.245	1.421 ± 0.271	1.300 ± 0.145

Table 2

Equilibrium Swelling Ratio (q) and Water Content (H) of SELP-47K Films

	MeOH-treated	MeOH-GTA-treated
q	2.06 ± 0.09	1.62 ± 0.12
H	51.35 ± 2.13	38.02 ± 4.74

Table 3

Attenuation Coefficients (α, cm^{-1}) of Hydrated SELP-47K Films

	nontreated	MeOH-treated	MeOH-GTA-treated
at 450 nm	1.58	1.30	12.89
at 350 nm	1.51	1.58	25.02

Table 4

Refractive Indices of SELP-47K Films Measured at Different Wavelengths

	532 nm	633 nm	1554 nm
nontreated	1.5345 ± 0.0025	1.5300 ± 0.002	1.5128 ± 0.0018
MeOH-treated	1.5366 ± 0.0047	1.5345 ± 0.0039	1.5181 ± 0.0031
MeOH-GTA-treated	1.5413 ± 0.0021	1.5399 ± 0.0043	1.5264 ± 0.0024

Table 5

Percentages of Secondary Structures As Determined by Curve Fitting of the Amide I Bands of SELP-47K Films

	aggregated strands	*β*-sheets	*β*-turns	unordered structure
nontreated	22.0	46.6	15.5	15.8
MeOH-treated	38.1	36.2	13.1	12.7
MeOH-GTA-treated	40.4	29.8	15.2	14.6